Heliyon 5 (2019) e01630

Contents lists available at ScienceDirect

Heliyon

journal homepage: www.heliyon.com

Three-dimensional model of DEMO-FNS facility considering neutronics and radiation shield problems

A.V. Zhirkin [*], B.V. Kuteev

National Research Center Kurchatov Institute (NRC KI), 1 Academician Kurchatov Square, 123182 Moscow, Russia

ARTICLE INFO

Keywords:
Atomic physics
Energy
Nuclear engineering
Nuclear physics

ABSTRACT

Recent neutronics studies of blankets for tokamak-based demonstration fusion neutron source (DEMO-FNS) showed a crucial influence of coolant composition on the transmutation rate of transuranic elements and tritium breeding in the system. The coolant choice varies with the neutron spectrum and shielding properties of the blanket. This paper presents a three-dimensional model developed for the Monte Carlo calculations of DEMO-FNS neutronics. The model was used for estimating the capability of the radiation shield to protect the superconducting electromagnetic system (EMS) from neutrons and gamma radiation for two types of coolants, namely water and supercritical carbon dioxide. The neutron balance, neutron energy spectra, and energy release of the neutrons and gamma radiation were evaluated in the shield, case, and superconductor at the inner and outer contours of the EMS. In comparison with the closed shielding option, the radiation heating power at the case and superconductor of the outer contour located between the injection port (IP) and the blanket maintenance port was 10 times higher than that in the area facing the injector. Thus, further improvement of the local shield design near the IP is needed.

1. Introduction

Tokamak plasma of the DEMO-FNS is a powerful generator of neutron flux and gamma radiation. The expected fusion power of the FNS tokamak has to be ~40 MW [1, 2, 3, 4, 5, 6, 7]. This value corresponds to the expected source neutron yield of 1.4×10^{19} n/s.

The radiation safety and shielding are key FNS problems and have a significant impact on the design and cost of the facility. The design of the radiation shield should be performed considering the development of other systems of the facility. The FNS blanket provides shielding properties in addition to those provided by the bulk radiation shield, which reduces the radiation fluence of magnetic coils and other elements of FNS to permissible values.

The spectrum of neutron and secondary photon radiation is formed in the blanket as a result of the absorption and generation of neutrons in its materials. The coolant composition is an important factor in the formation of blanket properties such as being a shield and a neutron generator.

Water is a typical shielding material. Using water as the blanket coolant enhances its shielding properties against neutrons. When water is replaced by another type of coolant, the protective capabilities of the blanket and the neutron radiation spectrum change significantly.

This paper is devoted to the analysis of sensitivity of the FNS shield characteristics to the coolant type.

2. Background

Currently, carbon dioxide is a prospective blanket coolant for the regions of transmutation and tritium breeding. According to preliminary estimations, replacement of water as a coolant by carbon dioxide significantly increases the rate of transmutations of minor actinides in the spent nuclear fuel of the blanket and ensures sufficient tritium generation for the self-supply of the device.

However, when water is replaced with the carbon dioxide as a coolant, the blanket neutron energy spectrum becomes significantly harder. The objective of this research is to estimate the capabilities of the EMS as a shield against neutrons and gamma radiation.

The studies were carried out using the Monte Carlo MCNP-4 code [8] with the cross-section nuclear data from the FENDL-2 [9] and ENDF/B-6 files [10].

3. Model

The three-dimensional model of the device is shown in Figs. 1 and 2 and in Tables 1 and 2. The main design elements of DEMO-FNS include the magnetic system, vacuum chamber, the first wall, blanket, thermal shield, and cryostat, the parameters of which are described in Ref. [8].

The volumetric source is presented as an elliptical torus. It emits D-T

---

[*] Corresponding author.
E-mail address: aleksej-zhirkin@yandex.ru (A.V. Zhirkin).

https://doi.org/10.1016/j.heliyon.2019.e01630
Received 30 January 2019; Received in revised form 1 March 2019; Accepted 30 April 2019
2405-8440/© 2019 Published by Elsevier Ltd. This is an open access article under the CC BY-NC-ND license (http://creativecommons.org/licenses/by-nc-nd/4.0/).

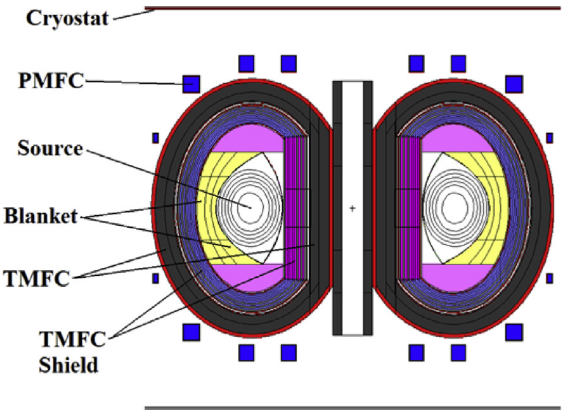

Fig. 1. View of the horizontal equatorial cross-section of the DEMO-FNS model.

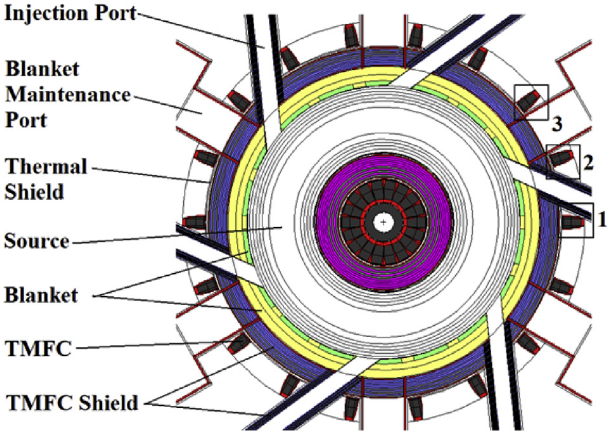

Fig. 2. View of the central vertical cross-section of the DEMO-FNS model.

Table 1
Composition of the mixture of oxides of minor actinides with the density of 9 g/cm^3.

Chemical element	Mass fraction, %
93-Np(237)O_2	44.5
95-Am(241)O_2	48.6
95-Am(242m)O_2	0.04
95-Am(243)O_2	6.1
96-Cm(243)O_2	0.02
96-Cm(244)O_2	0.74

neutrons with the energy of 14.1 MeV and has an isotropic angular distribution. The source neutron yield is 1.4×10^{19} n/s (the corresponding fusion power of the device is 40 MW). It has a linear space distribution along the equatorial radius.

The vacuum vessel consists of two steel shells; the radiation shield is inside these shells (Fig. 3).

The shield of the toroidal magnetic field coils is placed inside the vacuum chamber. The shield thickness together with the thickness of the walls of the vacuum chamber is equal to 72 cm along the inner perimeter of the coils and 60 cm on the outer perimeter.

The blanket consists of two sections. The first section (the nuclear zone) is used for transmutations and contains a minor actinide composition of NpO_2, AmO_2, and CmO_2. The second section (the breeding zone) is used to produce tritium from lithium orthosilicate (Li_4SiO_4) enriched with ^{6}Li isotope up to 90 % by mass.

Each section is presented in the form of a homogeneous layer which has the following composition:

Table 2
Components and parameters of the DEMO-FNS model.

Component	Parameters
Whole device	Equatorial radius – 630 cm height – 809 cm
Source (external surface)	Major radius – 320 cm semi-major axis – 120 cm semi-minor axis – 100 cm
The first wall	3 mm Be 1 mm Cu-Cr-Zr 3 mm H2O 1 mm SS316LN
Central solenoid	Nb3Sn Outer radius – 59.5 cm inner radius – 32.7 cm height – 528.8 cm
Vacuum vessel	Height – 651 cm.
Parameters on inner perimeter	Maximum radius – 213 cm, minimum radius – 141 cm.
Parameters on outer perimeter	Maximum radius – 551 cm, minimum radius – 491 cm.
Walls	SS316LN. Thickness – 3 cm.
Poloidal magnetic field coil	Number – 8. NbTi. Case – SS316LN.
Toroidal magnetic field coil (TMFC)	Number – 18, Nb3Sn. Case – SS316LN. Equatorial cross section: length – 71 cm, width – 39 cm.
TMFC shield	70 % vol. SS304B7, 30% vol. H_2O. Thickness on inner perimeter – 66 cm, thickness on outer perimeter – 54 cm.
Blanket	Height – 400 cm. Thickness of transmutation zone in equatorial cross-section – 15 cm. Thickness of breeding zone in equatorial cross-section – 20 cm.
Blanket maintenance port (BMP)	Number – 6 Width – 130 cm, height – 200 cm
Injection port (IP)	Number – 6. Width – 50 cm height – 100 cm
Local shield of IP	70 % vol. SS304B7, 30% vol. H_2O Thickness – 20 cm
Vacuum pumping port	18 at the top, 18 at the bottom. Diameter – 30 cm

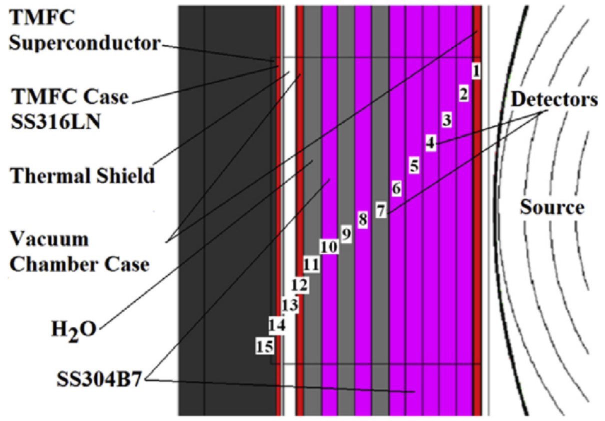

Fig. 3. Location of the detectors in the EMS shield, case, and superconductor on the internal contour of TMFC.

1. A mixture of oxides of minor actinides (79.0% vol.) (see Table 1) and coolant (21% vol.);
2. A layer of lithium orthosilicate Li_4SiO_4 (88% vol.), steel (5% vol.), and coolant (7% vol.).

Water was a coolant and moderator in the first calculation variant, and carbon dioxide with the density of 0.1 g/cm^3, at a temperature of approximately 200 °C and pressure of 80 kg/cm^2 is the coolant in the second.

There are three locations of TMFC (Fig. 2): 1– near the IP, 2– between the IP and the BMP, 3– near the BMP.

4. Results & Discussion

The locations of the volumetric detectors in the EMS shield and TMFC are shown in Figs. 3 and 4. The calculation results of neutron flux per 1 D-T neutron and energy release from neutrons and secondary photons for the source yield of 1.4×10^{19} n/s averaged over the detectors are shown in Figs. 5, 6, 7, and 8.

The neutron balance is shown in Table 3. The statistical uncertainty of the results in Table 3 is 0.2 %.

The amount of coolant sufficient to remove the heat generated in the blanket was estimated for water. The volume fraction of the coolant in the blanket refers to the water coolant. The same volume fraction was used for carbon dioxide. In general, the transition from a liquid to a gaseous coolant requires a larger volume. An increase of the carbon dioxide volume fraction affects both the shielding capability of the blanket and its neutronics performances. The minimal volume fraction of carbon dioxide in the system with the minimal influence on the shielding and performance was adopted.

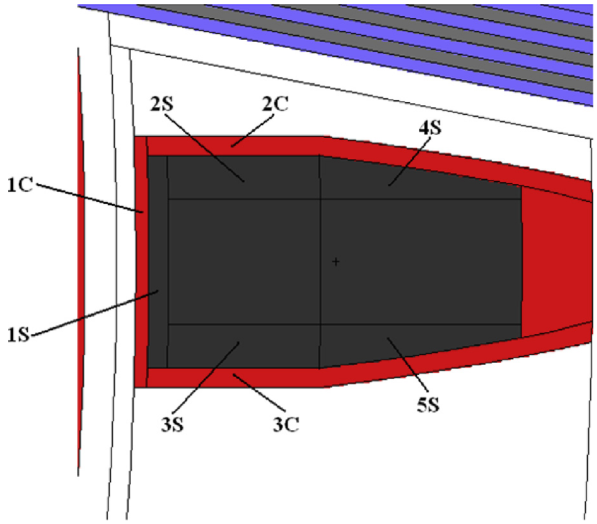

Fig. 4. Location of the detectors in the case (marked C) and superconductor (marked S) on the external contour of TMFC.

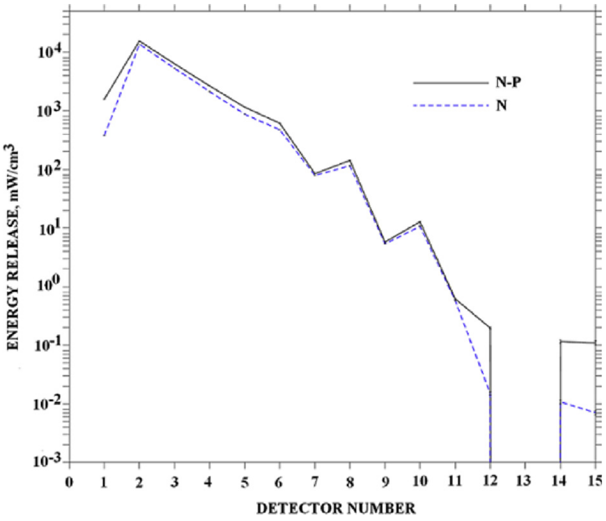

Fig. 5. Neutron energy release (N) and the neutron and secondary photon energy release (N-P) in the radiation shield, case, and superconductor on the internal contour of TMFC.

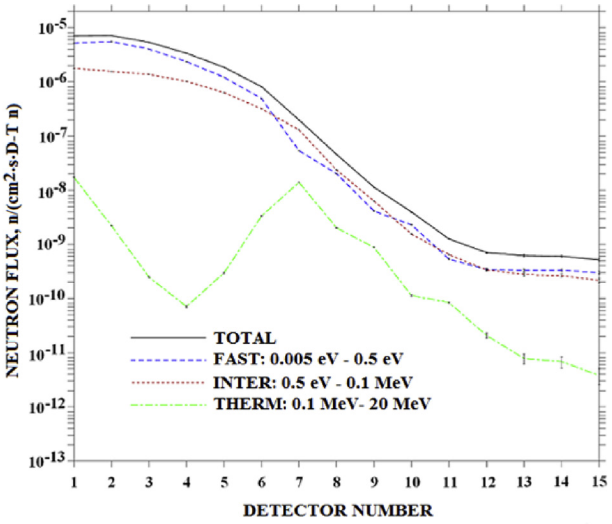

Fig. 6. Neutron flux density distribution for the basic energy groups in the radiation shield, case, and superconductor on the internal contour of TMFC.

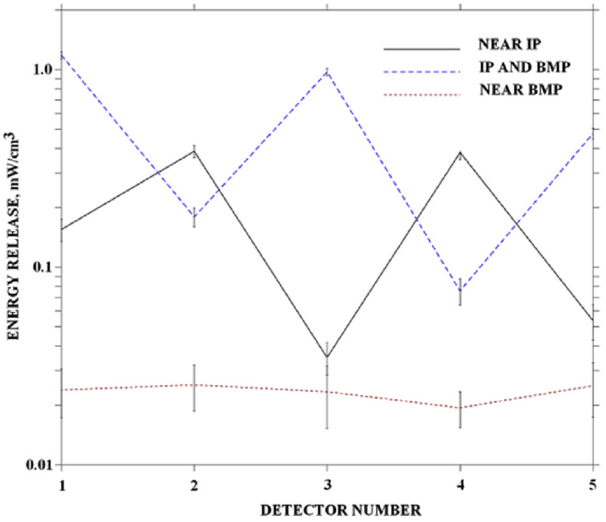

Fig. 7. Neutron and secondary photon energy release in the superconductor on the external contour of TMFC located near the IP, between the IP, and the BMP, and near the BMP.

According to Table 3, the total rate of the neutron generation to one D-T neutron three times greater (from 3.825 to 11.30) when replacing water with the carbon dioxide as the coolant.

The obtained results are explained by the fact that the neutron spectrum is harder in the blanket with carbon dioxide as a coolant, compared to water. The generation of fission neutrons in minor actinides is more active in the fast part of the spectrum, where the neutron yield to one fission reaction is significantly higher than that in the thermal region.

The blanket with the carbon dioxide coolant is a more powerful fast neutron source than the blanket with water as a coolant. This validates verification of shielding EMS in the changed neutron field.

The results in Figs. 5, 6, 7, and 8 show that the total energy release from neutrons and secondary photons in the case and superconductor on the internal and external contour of TMFC behind the monolithic iron-water shield (70% SS304B7 and 30% H_2O) is equal to 0.1 mW/cm^3, which is an acceptable result. The attenuation factor of the fast neutron flux density for the monolithic iron-water shield on the internal and

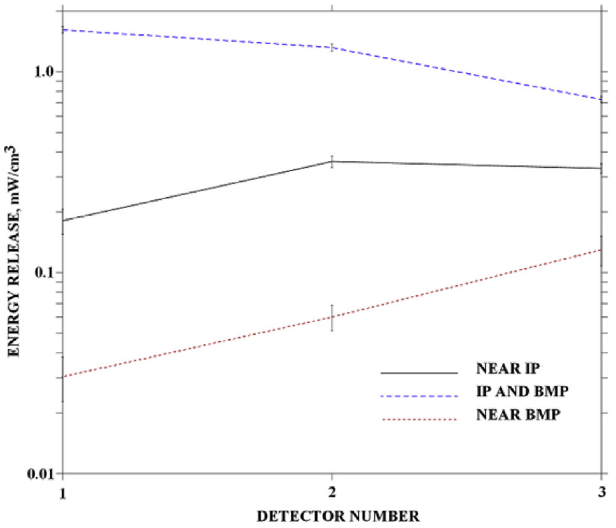

Fig. 8. Neutron and secondary photon energy release in the case on the external contour of TMFC located near the IP, between the IP and the BMP, and near the BMP.

Table 3
Balance of neutrons for the DEMO-FNS calculational models with the different coolants. (n,f) refers to fission reaction, (n,xn) is the sum of the reactions (n,2n), (n,3n), and so on.

	Coolant			
	H_2O		CO_2	
Process	Neutron generation	Neutron loss	Neutron generation	Neutron loss
Source	1	–	1	–
Absoption	–	2.878	–	7.790
(n,xn)	$4.353 \cdot 10^{-1}$	$2.102 \cdot 10^{-1}$	$4.994 \cdot 10^{-1}$	$2.423 \cdot 10^{-1}$
(n,f)	2.390	$7.364 \cdot 10^{-1}$	9.805	3.269
Leakage	–	$4.042 \cdot 10^{-5}$	–	$6.650 \cdot 10^{-5}$
Total	3.825	3.825	11.304	11.301

external contours satisfied the design limit of 1×10^3. The total energy release in the case and superconductor on the external contour of the EMS located between the IP and the BMP is too high in the area facing the IP and is equal to ~1.5 and ~1.0 mW/cm^3, respectively. The installed design limit for this value is 1.0 mW/cm^3. Given that the uncertainty of the calculational results should be at least half of this value, this indicates a significant influence of the IP on the energy release from neutron and secondary photon radiation in TMFC due to the insufficient thickness of the local iron-water shield of the IP, which is equal to 20 cm.

The ability of this model to reinforce the local shield of the IP is very limited. This raises the question of increasing the radial size of the device, which leads to a revision of the entire reactor design.

Declarations

Author contribution statement

A.V. Zhirkin: Performed the experiments; Analyzed and interpreted the data; Contributed reagents, materials, analysis tools or data; Wrote the paper.

B.V.Kuteev: Conceived and designed the experiments; Analyzed and interpreted the data.

Funding statement

This work was supported by State Atomic Energy Corporation Rosatom (N.4x.241.9B.17.1010).

Competing interest statement

The authors declare no conflict of interest.

Additional information

No additional information is available for this paper.

References

[1] E.A. Azizov, G.G. Gladush, A.V. Lopatkin, I.B. Lukasevich, Tokamak based hybrid systems for fuel production and recovery from spent nuclear fuel, Atom. Energy 110 (2) (2011) 93–98.

[2] E.P. Velikhov, E.A. Azizov, On Russian Strategy for Controlled Fusion, MFERW, Princeton, NJ, USA, 2011. Sept. 7–10.

[3] B.V. Kuteev, et al., Development of DEMO-FNS tokamak for fusion and hybrid technologies, Nucl. *Fusion* 55 (7) (2015) 073035.

[4] B.V. Kuteev, Y.S. Shpanskiy, Status of DEMO-FNS Development, IAEA, Vienna, 2017. April.

[5] E.A. Azizov, P.N. Alexeev, B.V. Kuteev, Update of Russian federation roadmap, in: 2nd IAEA DEMO Programme Workshop, 2013. Vienna, Austria, 17–20 December.

[6] B.V. Kuteev, et al., Intense fusion neutron sources, Plasma Phys. Rep. 36 (2010) 281.

[7] Development of technical design of fusion neutron source (FNS) with fusion power at least 10 MW. Stage of 2016. Report on research and development. Stage 2 (final). Inventory Number: NRC "Kurchatov Institute" 110.8-13/7133-16.

[8] J.F. Briesmeister (Ed.), MCNP—**A General Monte Carlo N-Particle Transport Code**, *Version 4C. LA-13709-M*, Los Alamos National Laboratory, 2000.

[9] D.L. Aldama, A. Trkov, FENDL-2.1. — Evaluated Nuclear Data Library for Fusion Applications, 467, INDC (NDS), 2004.

[10] R.F. Rose, C.L. Dunford, BNL-NCS-44945 (ENDF-102), revision 10/91. — *ENDF-102 Data Formats And Procedures For the Evaluated Nuclear Data File ENDF-6*, 1991. October.